ICIC Express Letters
Volume **15**, Number **7**, July **2021**

ICIC International ©2021 ISSN 1881-803X
pp. **681–691**

AMNIOTIC FLUID CLASSIFICATION BASED ON VOLUME AND ECHOGENICITY USING SINGLE DEEP POCKET AND TEXTURE FEATURE

Putu Desiana Wulaning Ayu[1,4], Sri Hartati[2,*], Aina Musdholifah[2] and Detty S Nurdiati[3]

[1]Doctoral Program, Department of Computer Science and Electronics
[2]Department of Computer Science and Electronics
Faculty of Mathematics and Natural Sciences
[3]Department of Obstetrics and Gynecology
Faculty of Medicine
Universitas Gadjah Mada
North Sekip, Bulaksumur, Yogyakarta 55281, Indonesia
*Corresponding author: shartati@ugm.ac.id; { aina_m; detty }@ugm.ac.id

[4]Department of Information Technology
Faculty of Computer and Informatics
Institut Teknologi Dan Bisnis STIKOM Bali
Raya Puputan No. 86, Denpasar 80234, Indonesia
wulaning_ayu@stikom-bali.ac.id

Received October 2020; accepted January 2021

Abstract. *The amniotic cavity contains fluid that serves as a cushion for the growing fetus and prevents its collision with the uterine wall. The amniotic fluid observation is a routine program performed by obstetricians to determine the growth of fetal health. However, in diagnose echogenicity, there are still differences in perceptions between obstetricians. Concerning these problems, this study proposes a feature extraction model and classification of amniotic fluid types into normal echogenic, normal clear, oligohydramnios echogenic, oligohydramnios clear, and polyhydramnios clear. The proposed feature extraction adopts obstetrician's knowledge or techniques in measuring volume using the Single Deep Pocket (SDP) method. Furthermore, it proposes a texture feature using First Order Statistical (FOS) and Gray Level Co-occurrence Matrices (GLCM) for echogenicity. In addition, the oversampling method was conducted due to the limited availability of data samples, while the experiments were performed using initial image data of 92 b-mode ultrasonography amniotic fluid. The classification stage used the SVM method, which was analyzed on three different kernels, namely RBF, polynomial, and sigmoid. The results showed that the proposed feature with RBF kernel can achieve an average value for an accuracy of 81.4%, precision of 80.8%, recall of 81.4%, F-measure of 81%, and ROC of 0.88.*

Keywords: Amniotic fluid, Echogenicity, Single deep pocket feature, Texture feature, Classification

1. **Introduction.** Amniocentesis or medical examination during pregnancy aims to determine the volume and condition of amniotic fluid, which is categorized into normal echogenic, normal clear, oligohydramnios echogenic, oligohydramnios clear, and polyhydramnios clear. Oligohydramnios is a condition characterized by a deficiency of amniotic fluid, which may inhibit fetal movement, formation, and cause intrauterine death. On the contrary, polyhydramnios is a pathological increase in the fluid volume, which may result in preterm labor, fetal macrosomia, malposition, and an increased risk of pregnancy disorders [1]. Furthermore, echogenic conditions may be associated with amniotic

DOI: 10.24507/icicel.15.07.681

fluid conditions containing meconium or vernix caseosa [2]. The presence raises concerns among doctors regarding fetal distress, the ability to tolerate birth, and even death [3]. Meanwhile, when the condition is clear, the overall color of the fluid is lucent or black which indicates the absence of fetal distress. Currently, obstetricians use the Single Deep Pocket (SDP) method to identify the amniotic fluid volume [4]. This method finds and determines the largest sac of amniotic fluid and conducts the measurement. Meanwhile, to diagnose echogenic or visually clear conditions diagnosis was conducted based on the gray intensity or opach area of the fluid. Visual observation was conducted when the amniotic fluid area has an opach or gray patch and may be categorized as echogenic because of its similarity with the placenta. However, the entire color is lucent or black when the fluid is clear. The lack of a standard for determining clear and echogenic categories is subject to different perceptions and screening results when observing the echogenicity.

To obtain a proper classification, it is necessary to have precise features to represent the amniotic fluid category. The case of amniotic fluid classification, both in the fields of computer vision and medical informatics, is still very rarely raised, and has never been studied before. Therefore, the literature review used is related to previous studies using objects or organs in ultrasonography images. The characteristics of the images are almost similar in some cases and this is evident in the fetal b-mode ultrasound imaging of the placenta, gestational sac, abdominal, and head. For segmentation phase, deep learning is one of most powerful approaches that provide satisfactory results. Looney et al. [5] proposed a fully convolutional Neural Network (OxNNet) to segment placenta from 3D Ultrasound (3D-US) volumes. The model combined deep convolutional neural network with random walk algorithm and used 300 ultrasonic images for training, verification, and testing, showing that the convolutional neural network can automatically segment the placenta in 3D ultrasound images. Han et al. [6] proposed an automatic segmentation method of human placenta using U-net architecture to reduce manual intervention and greatly speed up the segmentation, making large-scale segmentation possible.

In other work some studies proposed a method for classification of organ or tissue in ultrasound images. Liu et al. [7] conducted a study where b-mode placenta ultrasonography was classified by applying basic features to placental images, such as gray-level statistical features and tree multi-classification SVM to achieve an accuracy of 92%. Lei et al. [8] proposed a new method to automatically grade placental maturity from B-mode Ultrasound (BUS) and Color Doppler Energy (CDE) images based on a hybrid learning architecture. These methods can achieve remarkable performance for placental maturity evaluation. In other work, gray-scale intensity from B-mode Ultrasound (US) images and blood flow information from Color Doppler Energy (CDE) images by the visual feature detector and descriptor proposed by Li et al. [9]. After fusing information, they apply the feature encoding method, a Multi-layout Fisher Vector (MFV), to improving the staging performance. Meanwhile, Malathi and Shanthi [10,11] in 2010, classified the placenta into two classes, namely normal and abnormal by combining texture features of a histogram and Gray Level Co-occurrence Matrices (GLCM). In 2014, Lei et al. [12] performed automatic grading of placental maturity based on the Local Intensity Order Pattern (LIOP) and fisher vector feature.

In addition to the placenta, fetal head is one organ which also becomes the object of several studies. Furthermore, Ni et al. [13] and Li et al. [14], performed automatic measurements of fetal head, circumference using the Haar-like feature to represent the appearance of the anatomical structures. In 2017, Jang et al. [15] performed automatic measurements to obtain fetal abdominal circumference on b-mode ultrasonography images. Pradipta and Ayu [16] performed fetal weight prediction based on Biparietal Diameter (BPD) and Abdomen Circumference (AC) using iterative random Hough transform method. Similarly, Khazendar et al. [17] and Ibrahim et al. [18] conducted segmentation to apply shape features with an ellipsoidal algorithm approach to obtaining the Mean Sac

Diameter (MSD). The features of shape, spectral, geometry, and texture used for classification and segmentation of b-mode fetal ultrasound imaging are very diverse. Meanwhile, a study related to the features of b-mode ultrasonography amniotic fluid has never been conducted. Therefore, the determination of the exact features greatly influences the results of the volume and echogenic classification of the amniotic fluid by the classifier.

This study focuses on extraction to obtain features that represent fluid volume and echogenicity. Furthermore, it uses the shape or the Single Deep Pocket (SDP) feature to vertically search for the deepest area based on pixels representing the amniotic fluid. It also uses the texture features, including the Gray Level Co-occurrence Matrices (GLCM) and First Order Statistical (FOS) feature to obtain the echogenicity fluid value. Therefore, this study aims to classify the amniotic fluid conditions based on a combination of SDP and texture features. The main contributions of this study are: 1) The problems of this study are novel areas of processing and computer vision in medical images. This is evident in objects using b-mode ultrasonography to classify the conditions of amniotic fluid. 2) The SDP method proposed is a novel feature adopted from the current knowledge or techniques practiced by paramedics. Based on the experimental results, using a combination of SDP, FOS and GLCM features achieved average accuracy, precision, recall, F-measure, and ROC of 81.4%, 80.8%, 81.4%, 81%, and 0.88 respectively using SVM RBF.

The remaining part of this research is organized as follows. Section 2 explains the general proposed methods such as feature extraction, classifier, and performed measure. Section 3 contains experiment and result in an analysis of the proposed method, and Section 4 concludes the research.

2. **Method.**

This section describes the model for amniotic fluid classification, which primarily consists of image acquisition and pre-processing, segmentation, feature extraction, and classification.

2.1. **Image acquisition and pre-processing.**

When recording images, b-mode ultrasound amniotic fluid images are recorded by an ultrasound machine. In this study, 92 images consisting of 5 categories were used. The categories of these days include normal echogenic, normal clear, oligohydramnios echogenic, oligohydramnios clear, and polyhydramnios clear as shown in Figure 1. Furthermore, amniotic fluid images were obtained from the Obstetrics and Gynaecology laboratory of the Surya Husadha Hospital, Bali. The specifications of the machine used were accuvix XG and transducer with a frequency range of 3-3.5 Hz, the lateral resolution of 3 mm to 0.2 mm, image format in the form of jpg, and a size of 800 × 600 pixels. The gestational age used as data entered the second trimester during the 13th week. Furthermore, the image data used did not include pregnant women that were obese.

(a) (b) (c) (d) (e)

FIGURE 1. Amniotic fluid sample images of a (a) normal echogenic, (b) normal clear, (c) oligohydramnios echogenic, (d) oligohydramnios clear, and (e) polyhydramnios clear

2.2. **Segmentation.** The segmentation stage aims to obtain the Region of Interest (ROI) from the amniotic fluid area. This was achieved through the method of pixel classification scheme [19] based on our previous studies. The results produced several regions of amniotic fluid because the location in the ultrasound image is not specified. Therefore, the calculation for the number of fluid regions (counting) needs to be performed. When there is more than one region, the area segmented into an amniotic fluid is calculated. To validate the real ROI of the liquid, the region with the maximum area value is selected. After this process is complete, a morphological dilation operation follows to remove small objects in the ROI area that appear due to the presence of several pixels which may be noise or opach in amniotic fluid. Some examples of segmentation results are shown in Figure 2. At the acquisition stage, two obstetricians also performed labelling for the category and creating ground-truth images. At the pre-processing stage, an image cropping process was conducted to remove text information and re-size to 744×522 pixels.

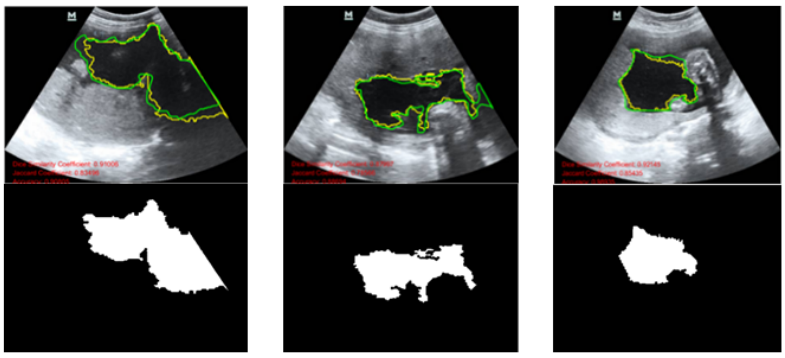

FIGURE 2. Upper row: edge detection for the amniotic fluid area. Bottom row: segmentation.

2.3. **Feature extraction.** This study uses the SDP and texture feature approach with GLCM combined with FOS feature. The SDP identified the type of amniotic fluid based on volume and texture feature used in the echogenicity.

2.3.1. *Texture feature using Gray Level Co-occurrence Matrices (GLCM).* The first feature extraction method uses GLCM, and it is a statistical method for examining textures and their spatial relationships. This method characterizes the texture of an image by counting the frequency of the appearance of the pixel pairs with certain values and spatial relationships in the image. The steps to obtain the texture features on GLCM are (1) image transformation into grayscale form, (2) co-occurrence matrix creation, (3) symmetrical matrix formation, and (4) normalization, which produce 22 texture features, such as autocorrelation, contrast, correlation1, correlation2, cluster prominence, cluster shade, dissimilarity, energy, entropy, homogeneity1, homogeneity2, maximum probability, sum of squares, sum average, sum entropy, sum variance, difference variance, difference entropy, information measure of correlation1 and 2, inverse difference normalized, inverse difference moment normalized [20].

2.3.2. *Texture feature using First Order Statistical (FOS).* Texture feature using FOS is a calculation conducted by using the original image pixel value to obtain the intensity distribution. In statistical results, it produces several features such as mean, skewness, entropy, kurtosis, standard deviation, and variance. Some of them are shown in Equations (1)-(6), where n is the row of the window, m is columns of the window, $h_{(i)}$ represents the total number of pixels with intensity level (i), N is the total number of pixels with $N = n \times m$, and G is the maximum gray-level.

$$\text{Mean: } \bar{x} = \sum_{n} \sum_{m} \sum_{i=0}^{G-1} i_{(n,m)} P_{(n,m)} \tag{1}$$

$$\text{Skewness: } \bar{x}_3 = \sigma^{-3} \sum_{n} \sum_{m} \sum_{i=0}^{G-1} \left(i_{(n,m)} - \bar{x}\right)^3 P_{(n,m)} \tag{2}$$

$$\text{Standard deviation: } S = \sqrt{\frac{1}{N-1} \sum_{n} \sum_{m} \left(x_{(n,m)} - \bar{x}\right)^2} \tag{3}$$

$$\text{Variance: } S = \frac{1}{N-1} \sum_{n} \sum_{m} \left(x_{(n,m)} - \bar{x}\right)^2 \tag{4}$$

$$\text{Entropy: } H = \sum_{n} \sum_{m} \sum_{i=0}^{G-1} P_{(n,m)} \log_2 \left[P_{(n,m)}\right] \tag{5}$$

$$\text{Kurtosis: } \bar{x}_4 = \sigma^{-4} \sum_{n} \sum_{m} \sum_{i=0}^{G-1} \left(i_{(n,m)} - \bar{x}\right)^4 P_{(n,m)} - 3 \tag{6}$$

2.3.3. *Single Deep Pocket (SDP) feature.* This feature is adopted from the way obstetricians categorize the volume of amniotic fluid. Conceptually, to obtain the SDP feature, the longest vertical line of the amniotic fluid is selected. Furthermore, the first stage of its extraction model is to find the bounding box of amniotic fluid ROI. The next is to create a matrix according to the size of the bounding box and convert it to binary form. The ROI area is converted to white (1) while the outside is converted to black (0). Meanwhile, the algorithm for obtaining the longest vertical and straight line is shown by the flowchart in Figure 3. Amniotic fluid ROI is a binary image in a matrix form that is processed based on columns and rows. The calculation is conducted by finding the column in the matrix with the highest value of 1 (white) which represents the amniotic fluid. The output of this algorithm is the number of pixels that have the highest number of values 1 and the index of the column. The stages of finding the SDP feature begin with initialization of the initial value, where $Max = 0$ is a variable to store the maximum value 1. Meanwhile, the column is a variable to store the index that has the most value 1. $Sum[k]$ is the variable to store the number of values 1 from each row and column, while m is the number of columns. Iteration in the calculation starts from column 1 and row 1 to row i (b_i). When the row and column are 1, the value of 1 will be added to the variable $sum[k]$. Conversely, when it is 0, the value is continued by checking the next row. After the iteration where rows become greater than n (number of rows), the value is continued by going to the next column and setting the maximum to $sum[k]$. In addition, the iteration in the next column is still the same, and this is evident in checking until the n row since the maximum value will change to $sum[k]$. When it is less than the $sum[k]$ value of column i, then, the maximum value has been updated to the highest number of 1. However, the iteration is only complete when the column is greater than m. Therefore, the output is maximum, and the column has the most pixel value 1 in m. The calculation process is expressed through the following Equation (7).

$$Max \sum_{c=1}^{n} \left[\sum_{r=1}^{n} x[c_i, r_i] = 1 \right] \tag{7}$$

c is the column of matrix and r represents row, and each of these two pair is denoted by $[c_i, r_i]$.

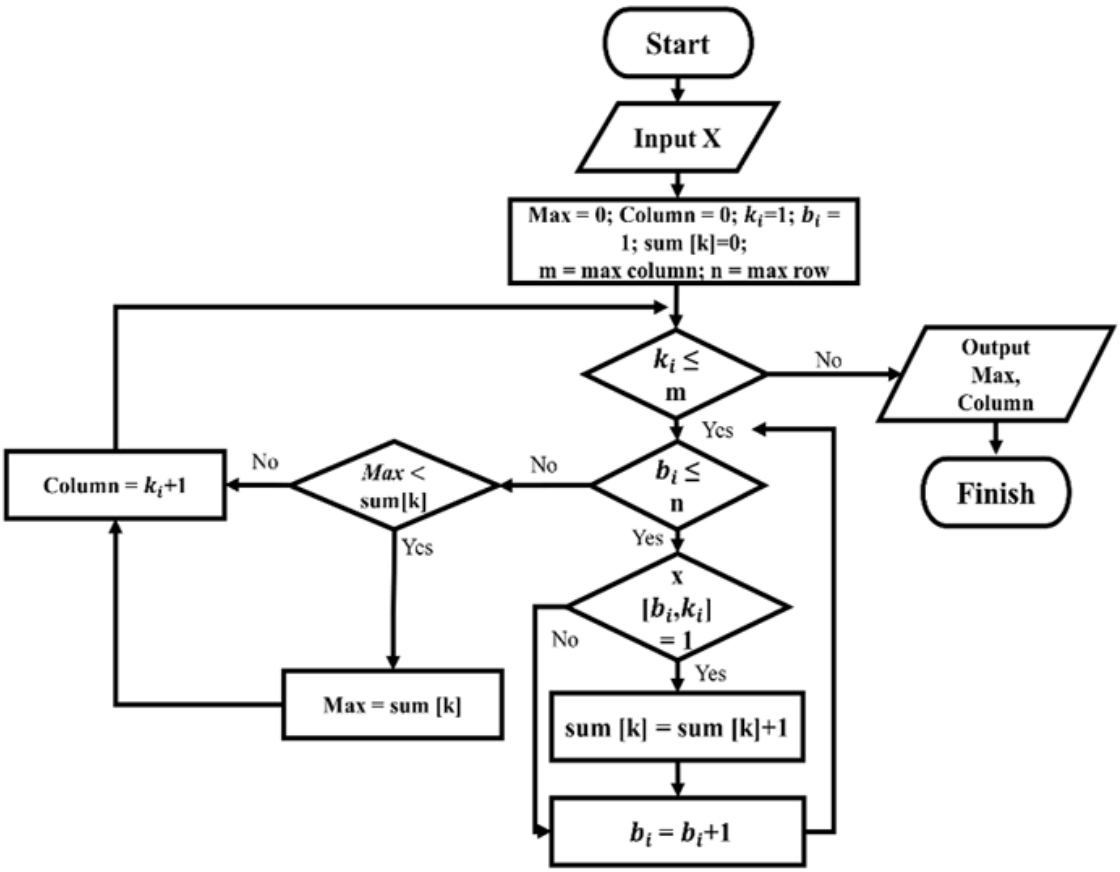

FIGURE 3. Flowchart of the proposed feature extraction method

2.4. **Classification.** Support Vector Machine (SVM) was chosen as a classification method because of its ability to minimize generalization errors [20]. The minimization is conducted by searching for and selecting the hyperplane with the largest margin. In addition, three kernels including the Radial Base Function (RBF), polynomial, and sigmoid were used in this study. The formula for each kernel is shown in Equations (8)-(10).

$$\text{RBF kernel: } K(x_i, x_j) = \exp\left(-\gamma \|x_i - x_j\|^2\right), \quad \gamma > 0 \tag{8}$$

$$\text{Polynomial kernel: } K(x_i, x_j) = \left(\gamma \cdot x_i^T \cdot x_j + r\right)^2, \quad \gamma > 0 \tag{9}$$

$$\text{Sigmoid kernel: } K(x_i, x_j) = \tanh\left(\gamma \cdot x_i^T \cdot x_j + r\right) \tag{10}$$

where $K(x_i, x_j)$: kernel; $\|x_i - x_j\|^2$: The squares of the Euclidean distance between x_i and x_j; γ: Gamma (distribution of the kernel).

Determining the value of the Gamma (γ) parameter is one of the aspects evaluated in the kernel because it is related to complexity and overfitting. Meanwhile, c (cost function) is a penalty for misclassifying data. The higher the value of c, the narrower the division of the decision area in each class. The cost function (c) for two kernels is set to 1, while the Gamma parameter (γ) is $1/n$ feature, where n feature is 95.

2.5. **Performance measure.** The parameters used to measure the performance of the classification model are accuracy, precision, recall, and F-measure as shown in Equations (11)-(14). In medical decision making, Receiver Operating Characteristic (ROC) curve is commonly used because of imbalanced class data, where ROC is a trade-off between the sensitivity (TP rate) and FP rate values. Furthermore, the ROC is used to measure the model accuracy [21].

$$\text{Accuracy} = \frac{\text{TP} + \text{TN}}{\text{TP} + \text{FP} + \text{TN} + \text{FN}} \tag{11}$$

$$\text{Recall} = \frac{\text{TP}}{\text{TP} + \text{FN}} \tag{12}$$

$$\text{Precision} = \frac{\text{TP}}{\text{TP} + \text{FP}} \tag{13}$$

$$\text{F-measure} = \frac{\text{Precision} \cdot \text{Recall}}{\text{Precision} + \text{Recall}} \tag{14}$$

TP is True Positive (a positive label that is predicted as an actual label), FP is False Positive (negative label but predicted as a positive label), TN is True Negative (negative data that predicted correctly), and FN is False Negative (a positive label but predicted as negative label).

3. Experiment and Result.

3.1. Performance result of the SVM method.

In this first experiment section, the classification stage used the SVM method, which analyzed three different kernels, namely RBF, polynomial, and sigmoid. Accuracy, precision, recall, F-measure, and ROC of the three kernels used all proposed features, and the performance is shown in Tables 1, 2, and 3. The validation is conducted using a *k-fold* cross, where the number $k = 3$. In addition, training and testing are divided into a ratio of 75 : 25, where they have a total of 69 and 23 data, respectively.

Table 1. Performance result of SVM RBF kernel with all proposed feature

SVM RBF kernel	Accuracy (%)	Precision (%)	Recall (%)	F-measure (%)	ROC
Normal echogenic	55	86	55	67	0.76
Normal clear	98	74	98	84	0.73
Oligohydramnios echogenic	0	0	0	0	0
Oligohydramnios normal	100	100	100	100	1
Polyhydramnios normal	0	0	0	0	0

Table 2. Performance result of SVM polynomial kernel with all proposed feature

SVM polynomial kernel	Accuracy (%)	Precision (%)	Recall (%)	F-measure (%)	ROC
Normal echogenic	27	86	27	41	0.63
Normal clear	98	68	98	81	0.65
Oligohydramnios echogenic	0	0	0	0	0
Oligohydramnios normal	100	83	100	91	0.99
Polyhydramnios normal	0	0	0	0	0

The results of the experiment showed that the performance of the SVM RBF kernel method obtained the highest values for accuracy, precision, recall, F-measure, and ROC compared to SVM polynomial and sigmoid kernel in each amniotic fluid class. Furthermore, the SVM RBF kernel achieved an average accuracy, precision, recall, and F-measure value of 77%, 52%, 51%, and 51% respectively. Also, it achieved an average ROC of 0.86 with a combination of 95 features. An analysis of the combination of features was conducted using the SVM RBF kernel, and its comparison results with several features are shown in Table 4. The combination of GLCM and SDP with 23 features produces performance with the highest average accuracy value of 74%, precision of 50%, recall of 48%,

Table 3. Performance result of SVM sigmoid kernel with all proposed feature

SVM sigmoid kernel	Accuracy (%)	Precision (%)	Recall (%)	F-measure (%)	ROC
Normal echogenic	47	88	32	47	0.65
Normal clear	98	64	98	78	0.59
Oligohydramnios echogenic	0	0	0	0	0
Oligohydramnios normal	0	0	0	0	0
Polyhydramnios normal	0	0	0	0	0

Table 4. Classification performance of SVM RBF kernel method by combination features

	Features	Total	Avg Acc (%)	Avg Pre (%)	Avg Recall (%)	Avg F-measure (%)	ROC Area
GLCM with several orientation + SDP	GLCM orientation 0° + SDP	23	74	50	48	48	0.84
	GLCM orientation 45° + SDP	23	60	22	23	21	0.75
	GLCM orientation 90° + SDP	23	64	25	27	25	0.78
	GLCM orientation 135° + SDP	23	67	42	46	43	0.80
FOS + SDP	Mean, Entropy, STD, Variance, Skewness, Kurtosis, Energy, SDP	7	68	48	31	33	0.80
GLCM + FOS + SDP	GLCM orientation 0° + FOS + SDP	29	76	52	50	49	0.85
	GLCM orientation 45° + FOS + SDP	29	61	42	26	26	0.76
	GLCM orientation 90° + FOS + SDP	29	62	25	23	22	0.76
	GLCM orientation 135° + FOS + SDP	29	67	45	44	43	0.80
All features (proposed method)	GLCM orientation 0° + 45° + 90° + 135° + FOS + SDP	**95**	**77**	**52**	**51**	**51**	**0.86**

F-measure of 48%, and ROC of 0.84 in GLCM orientation of 0°. Furthermore, the combination of FOS and SDP with a total feature of 7 produce performance with an average accuracy value of 68%, precision of 48%, recall of 31%, F-measure of 33%, and ROC of 0.8. Based on the overall classifier performance, it appears that all models fail to recognize the oligohydramnios echogenic and polyhydramnios normal classes. This is most likely due to the small number of train data in the class which results in the model not being able to recognize patterns from that class. Therefore, the second experiment was carried out to improve the classification results.

3.2. **Performance result of SVM RBF method after oversampling data.** The results in Tables 1, 2, and 3 show that classifier tends not to recognize or classify the normal classes of polyhydramnios and oligohydramnios echogenic. This is because the number of data representations is very small, and the classifier will be difficult to generalize the data. Therefore, the second experiment was conducted with the addition of oversampling stages to balance the amount of data in each class. The oversampling method involves creating new synthetic data which is typically used to solve imbalance problems. This study uses one of the most popular methods proposed by Chawla et al., which is the Synthetic Minority Oversampling Technique (SMOTE) [22]. SMOTE is a minority class oversampling method, in which several samples are taken, and the closest data points are determined with the standard number of 5 [22]. Additionally, new synthetic data is then generated along the interpolated lines of the sample points and their closest neighbors. Some studies use the SMOTE method to add data to the minority class. Pradipta et

al. [23] improved the performance of the ensemble multiclassifier method in classifying the umbilical cord organs. Meanwhile, other studies combine SMOTE for breast cancer identification and classification [24,25].

This second experiment uses the *k-fold cross-validation* method with the amount of $k = 3$. The training and testing consist of 206 and 69 data in the ratio of 75 : 25. The oversampling results balanced the data for each class by 55, on the ground that the total becomes 275. Based on the confusion matrix in Table 5, the performance of the classifier increases as seen in its ability to recognize polyhydramnios normal and oligohydramnios echogenic classes. However, without oversampling, the classifier cannot recognize these two classes at all. Table 6 showed that the classifier performance increased with an average accuracy value of 81.4%, precision of 80.8%, recall of 81.4%, F-measure of 81%, and ROC of 0.88. These results showed that the increasing number of data in the minority class of the dataset causes the classifier to identify and learn their various patterns. This increase in performance also demonstrates the ability of the classifier to generalize data and produce more optimal.

Table 5. Confusion matrix of SVM RBF kernel and SMOTE with all proposed feature

	Amniotic fluid	Output class					Total
		Normal echogenic	Normal clear	Oligohydramnios echogenic	Oligohydramnios normal	Polyhydramnios normal	
Target class	Normal echogenic	**45**	4	0	0	6	55
	Normal clear	10	**28**	8	0	9	55
	Oligo echogenic	0	6	**49**	0	0	55
	Oligo normal	0	0	0	**55**	0	55
	Polyhydramnios normal	1	6	0	1	**47**	55
	Total	56	44	57	56	62	**224**

Table 6. Performance result of SVM RBF kernel and SMOTE with all proposed feature

SVM RBF kernel + SMOTE	Accuracy (%)	Precision (%)	Recall (%)	F-measure (%)	ROC
Normal echogenic	81.8	80	82	81	0.88
Normal clear	50.9	64	51	57	0.72
Oligo echogenic	89	86	89	88	0.93
Oligo normal	100	98	100	99	1.0
Polyhydramnios normal	85.4	76	85	80	0.89

4. **Conclusions.** This study aims to identify features that classify the volume and echogenicity of amniotic fluid. For the first analysis and experiment, the result showed the combination for the 4 orientation angles of GLCM, FOS, and SDP feature with a total of 95 features has the corresponding highest average accuracy, precision, recall, F-measure, and ROC values, at 77%, 52%, 51%, 51%, and 0.86. Furthermore, the results in the first experiment showed that there was an imbalanced data condition. Due to this condition, the classifier failed to recognize the minority class of the data set. Based on these results, the second experiment was conducted with the addition of data oversampling stages in the polyhydramnios normal and oligohydramnios echogenic classes. Therefore, the number of data in each class was 55, while the total instantly became 275. This result with SVM RBF kernel on the combination of GLCM features at 4 angles orientation (0°, 45°, 90°, 135°), FOS, and SDP feature showed in Table 6 an increase in performance with the

average values of accuracy, precision, recall, F-measure, and ROC of 81.4%, 80.8%, 81.4%, 81%, and 0.88 respectively. For future work, to improve classification performance, we will add features and use images augmented to multiply the image dataset and will try rule-based classification methods.

REFERENCES

[1] L. Dallaire and M. Potier, *Amniotic Fluid*, 2nd Edition, Elsevier, 2012.

[2] G. Tam and T. Al-Dughaishi, Case report and literature review of very echogenic amniotic fluid at term and its clinical significance, *Oman Med. J.*, vol.28, no.6, pp.28-30, 2013.

[3] R. Mundhra and M. Agarwal, Fetal outcome in meconium stained deliveries, *J. Clin. Diagn. Res.*, vol.7, no.12, pp.2874-2876, 2013.

[4] S. Q. Rashid, Amniotic fluid volume assessment using the single deepest pocket technique in Bangladesh, *J. Med. Ultrasound*, vol.21, no.4, pp.202-206, 2013.

[5] P. Looney, G. N. Stevenson, K. Nicolaides et al., Fully automated, real-time 3D ultrasound segmentation to estimate first trimester placental volume using deep learning, *JCI Insight*, vol.3, no.11, 2018.

[6] M. Han, Y. Bao and Z. Sun, Automatic segmentation of human placenta images with U-Net, *IEEE Access*, vol.7, pp.180083-180092, 2019.

[7] Z. Liu, H. Zheng and S. Lin, Application of multi-classification support vector machine in the B-placenta image classification, *Proc. of 2009 Int. Conf. Comput. Intell. Softw. Eng. (CiSE2009)*, 2009.

[8] B. Lei, E. Tan and S. Chen, Automatic placental maturity grading via hybrid learning, *Neurocomputing*, vol.223, pp.86-102, 2017.

[9] W. Li, T. Wang, D. Ni, S. Chen, B. Lei and Y. Yao, Placental maturity evaluation via feature fusion and discriminative learning, *Chinese J. Biomed. Eng.*, vol.35, no.4, pp.411-418, 2016.

[10] G. Malathi and V. Shanthi, Histogram based classification of ultrasound images of placenta, *Int. J. Comput. Appl.*, vol.1, no.16, pp.58-61, 2010.

[11] G. Malathi and V. Shanthi, Statistical measurement of ultrasound placenta images using segmentation approach, *Proc. of 2010 Int. Conf. Signal Image Process. (ICSIP2010)*, pp.309-316, 2010.

[12] B. Lei, X. Li and Y. Yao, Automatic grading of placental maturity based on LIOP and fisher vector, *Int. Conf. IEEE Eng. Med. Biol. Soc. (EMBC2014)*, pp.4671-4674, 2014.

[13] D. Ni, Y. Yang and S. Li, Learning based automatic head detection and measurement from fetal ultrasound images via prior knowledge and imaging parameters, *Proc. of Int. Symp. Biomed. Imaging*, pp.772-775, 2013.

[14] J. Li, Y. Wang and B. Lei, Automatic fetal head circumference measurement in ultrasound using random forest and fast ellipse fitting, *IEEE J. Biomed. Heal. Informatics*, vol.22, no.1, pp.215-223, 2018.

[15] J. Jang, Y. Park, B. Kim, S. M. Lee, J.-Y. Kwon and J. K. Seo, Automatic estimation of fetal abdominal circumference from ultrasound images, *IEEE J. Biomed. Heal. Informatics*, vol.22, no.5, pp.1512-1520, DOI: 10.1109/JBHI.2017.2776116, 2018.

[16] G. A. Pradipta and P. D. W. Ayu, Fetal weight prediction based on ultrasound image using fuzzy c means clustering and iterative random Hough transform, *Proc. of 2017 the 1st Int. Conf. Informatics Comput. Sci. (ICICoS 2017)*, pp.71-76, 2018.

[17] S. Khazendar, J. Farren and H. Al-Assam, Automatic segmentation and classification of gestational sac based on mean sac diameter using medical ultrasound image, *Mob. Multimedia/Image Process. Secur. Appl.*, 2014.

[18] D. A. Ibrahim, H. Al-assam and S. Jassim, Multi-level trainable segmentation for measuring gestational and yolk sacs from ultrasound images, *Commun. Comput. Inf. Sci.*, pp.86-97, 2017.

[19] D. W. Ayu, S. Hartati and A. Musdholifah, Amniotic fluid segmentation by pixel classification in B-mode ultrasound image for computer assisted diagnosis, in *Int. Conf. Soft Comput. Data Sci.*, Singapore, Springer, 2019.

[20] M. Abdel-Nasser, J. Melendez, A. Moreno, O. A. Omer and D. Puig, Breast tumor classification in ultrasound images using texture analysis and super-resolution methods, *Eng. Appl. Artif. Intell.*, vol.59, pp.84-92, 2017.

[21] D. A. Tyas, S. Hartati, A. Harjoko and T. Ratnaningsih, Morphological, texture, and color feature analysis for erythrocyte classification in thalassemia cases, *IEEE Access*, vol.8, pp.69849-69860, 2020.

[22] N. V Chawla, K. W. Bowyer, L. O. Hall and W. P. Kegelmeyer, SMOTE: Synthetic minority oversampling technique, *J. Artif. Intell. Res.*, vol.16, pp.321-357, 2002.

[23] G. A. Pradipta, R. Wardoyo, A. Musdholifah and I. N. H. Sanjaya, Improving classifiaction performance of fetal umbilical cord using combination of SMOTE method and multiclassifier voting in imbalanced data and small dataset, *Int. J. Intell. Eng. Syst.*, vol.13, no.5, pp.441-454, 2020.

[24] D. Kaushik, B. R. Prasad, S. K. Sonbhadra and S. Agarwal, Post-surgical survival forecasting of breast cancer patient: A novel approach, *2018 Int. Conf. Adv. Comput. Commun. Informatics (ICACCI2018)*, pp.37-41, 2018.

[25] S. W. Purnami and R. K. Trapsilasiwi, SMOTE-least square support vector machine for classification of multiclass imbalanced data, *ACM Int. Conf. Proceeding Ser.*, pp.107-111, 2017.